ARTICLE

pH Effect on Oxidation of Hydrogen Peroxide on Au(111) Electrode in Alkaline Solutions

Jiao-jiao Li, Jie Wei, Jun Cai, Yan-xia Chen*

Hefei National Laboratory for Physical Sciences at the Microscale and Department of Chemical Physics, University of Science and Technology of China, Hefei 230026, China

The hydrogen peroxide oxidation reaction (HPOOR) on Au(111) electrode in alkaline solutions with pH values ranging from 10 to 13 was examined systematically. HPOOR activity increased and the slope of the i-E curve decreased with increasing pH. HO_2^- is suggested to be the main reactive intermediate for HPOOR in alkaline media. The fast kinetics for HPOOR in alkaline solution is facilitated by the electrostatic interaction between the positively charged electrode and the reactive anions (*i.e.*, HO_2^- and OH^-), which increases the concentration of these reactants and the thermodynamic driving force for HO_2^- oxidation at the reaction plane.

Key words: Oxidation of hydrogen peroxide, Au(111) electrode, pH effect, Electrostatic interaction

I. INTRODUCTION

The oxygen reduction reaction (ORR) is the primary cathodic reaction in fuel cells. Its high overpotential remains the most critical bottleneck restricting the commercialization of fuel cells [1–3]. For reactions such as ORR, which involves the transfer of protons and electrons, variation in the solution pH may have many effects on these reactions [2, 4, 5]: it may change (i) the thermodynamic equilibrium potential, (ii) the nature and concentration of the reactive species, (iii) the reaction kinetics of electrocatalytic reactions, and (iv) the surface properties, *e.g.* the type and the coverage of the adsorbate and the excess surface charge. Hence, studying the pH effect will provide rich information towards unravelling the reaction mechanism and identifying the most important factors.

Hydrogen peroxide (HPO) is one of the possible intermediates of ORR [1–3]. On Pt group or Pt-based electrocatalysts, there is a potential range in which ORR is under kinetic and mass transport mixed control. In this mixed potential region, both the oxidation and the reduction of HPO (denoted as HPOOR and HPORR hereafter) can occur [1, 6]. Understanding the mechanism and kinetics of HPOOR and HPORR will be of great help in understanding the mechanism and identifying the key factors governing the efficiency of ORR [2, 7–9]. However, it remains difficult to obtain a clear understanding of the structure-activity relationship of each reaction on such electrocatalysts. On Au electrodes, a very large overpotential is needed for HPORR to occur [2, 9], which leads to a large separation between the potential regions in which HPOOR and HPORR occur. Hence, the Au electrode is a good model system for studying the kinetics and mechanism of HPORR and HPOOR. To the best of our knowledge, only one study has examined HPOOR and HPORR on a Au electrode in acid solution at two different pH values (pH=1.2 and 4.0) [10]. This study found that at a constant pH, the HPOOR activity changes with electrode crystal orientation in the order Au(111)<Au(110)<Au(100). On all three types of electrodes and at high overpotentials (η>0.3 V), the HPOOR activity is smaller at pH=4.1 than pH=1.2, while the opposite trend is observed in the low overpotential region (η<0.3 V) on Au(111). This phenomenon is explained by invoking the site-blocking effect of OH_{ad}.

Until now, the pH effect on HPOOR and HPORR on Au(111) electrodes in alkaline solution has not been reported, in this study, the pH effect on HPOOR and HPORR on Au(111) in solutions with pH ranging from 10 to 13 is examined. We find that the HPORR activity is negligibly slow on Au(111) in all solutions examined. With the gradual increase of solution pH from 10 to 13, the HPOOR activity increases monotonically. Factors which determine HPOOR and HPORR kinetics on Au(111) will be discussed based on these findings.

II. EXPERIMENTS

Solutions with 0.5 mol/L $NaClO_4$+2 mmol/L H_2O_2+x mmol/L NaOH were prepared using 99% sodium perchlorate (Suprapure, Aladdin), 30% H_2O_2 (SSG, Wako Pure Chemical industries, Ltd.), 99%

_____

*Author to whom correspondence should be addressed. E-mail: yachen@ustc.edu.cn

sodium hydroxide (Suprapure, Sigma-Aldrich) and Milli-Q water (18.2 MΩ·cm). The working electrode (WE) Au(111) (diameter: 2.5 mm) was prepared by the Clavilier method [11]. The annealing and cleaning of the WE were carried out in the same procedure as described in Refs.[2, 7, 9]. A conventional two-compartment, three-electrode glass cell was used for all the electrochemical measurements. An Ag/AgCl electrode and an Au foil electrode were used as reference electrode (RE) and counter electrode (CE), respectively. A meniscus configuration was maintained between the Au(111) surface and the electrolyte during all measurements. The oxidation of H_2O_2 on Au(111) was investigated in N_2-saturated (99.999%, the Linde Group, China) solution by cyclic voltammetry using a hanging-meniscus rotating disk electrode (HMRDE) configuration at various electrode rotation speeds and a scan rate of 50 mV/s. The electrode rotation speed (ω) was controlled using a modulated rotator (Hokuto Denko Ltd.). All potentials in this work are quoted against the reversible hydrogen electrode (RHE).

III. RESULTS AND DISCUSSION

A. Characterization of the Au(111) electrode

The quality of the prepared Au(111) electrode was examined by cyclic voltammetry in N_2-saturated 0.1 mol/L H_2SO_4 (inset in FIG. 1). In the positive-going scan, small anodic currents at low potentials (<0.2 V) correspond to capacitive charging of the electrical double layer. Scanning of the electrode potential toward more positive potentials leads to the lifting of the thermally induced reconstruction, from Au(111)-p($\sqrt{3}\times\sqrt{3}$) to Au(111)-(1×1), which is represented in the voltammogram by the current peak at ca. 0.55 V. The broad feature in the potential region from 0.40 V to 0.80 V is attributed to the disordered adsorption of (hydrogen-) sulfate anions on Au(111)-(1×1). A disorder-order phase transition takes place within the sulfate adlayer upon reaching a critical coverage of 0.20 ML, as represented by the pair of sharp current peaks at ca. 1.05 V. The current-potential (i-E) features of the Au(111) electrode agree well with those reported in Refs.[12, 13], demonstrating the high quality of the Au(111) electrode employed in this study.

Before investigating the electrochemical behavior of HPOOR, the base cyclic voltammograms were also recorded in alkaline solutions without H_2O_2, as shown in FIG. 1. The small anodic current appearing in the positive-going scan from 0.3 V to 1.0 V comes from the discharge of OH^-, which leads to the formation of adsorbed OH (denoted as OH_{ad}). At an electrode potential $E>1.0$ V, surface oxidation of Au(111) takes place, with two anodic peaks appearing at ca. 1.1 V and 1.3 V, respectively. Reversing the scan direction at 1.5 V results in a rapid cessation of oxidation currents,
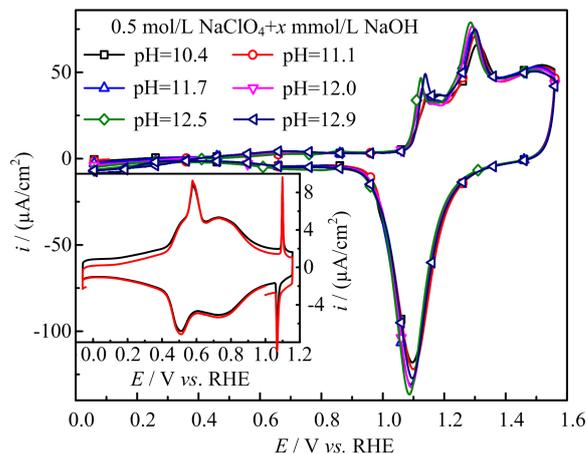

FIG. 1 Cyclic voltammograms of Au(111) electrode in 0.5 mol/L $NaClO_4$+x mmol/L NaOH solutions with different pH. Scan rate is 50 mV/s. Inset shows the CV for the same electrode recorded in 0.1 mol/L H_2SO_4.

followed by a cathodic peak at ca. 1.1 V, due to the reduction of three different gold oxides in different oxidation extent (Au^+, Au^{2+} and Au^{3+}) [10]. These features are quite similar to those reported in acidic media [10, 12, 13], except that the potential regime for the adsorption/desorption of OH and the oxidation/reduction of Au is negatively-shifted by ca. 60 mV compared with that in acidic media. The high OH^- concentration of the alkaline solutions used in the present study is suggested to be the origin of these changes. Furthermore, we find that the CV features of Au(111) in solutions with different pHs differing a little in the potential region with $E>1.0$ V for Au oxidation (FIG. 1(b)). This is probably due to the slight differences in the meniscus height, together with the high viscosity of the electrolyte, which leads to the involvement of different numbers of sites (most defects) on the edge in the electrochemical processes. We will demonstrate in a forthcoming work that due to the great difference in the HPOOR activity of Au(111) sites and defect sites at the edge, significant differences can be seen in the polarization curves for HPOOR. All these remind us that carefully controlling the meniscus height is of great importance in order to remove such effects when studying the effect of pH on the HPOOR on Au(111).

B. pH effect on HPOOR on Au(111) electrode

FIG. 2(a) displays the polarization curves for HPOOR on a Au(111) electrode in 0.1 mol/L NaOH at different electrode rotation speeds. In the positive-going scan from 0.5 V to 0.8 V, there is barely any current. HPOOR starts at $E>0.8$ V. The oxidation current increases with E and reaches a plateau at $E>0.9$ V. The onset potential for HPOOR being ca. 0.8 V, ca. 0.16 V more positive than its thermodynamic equilibrium
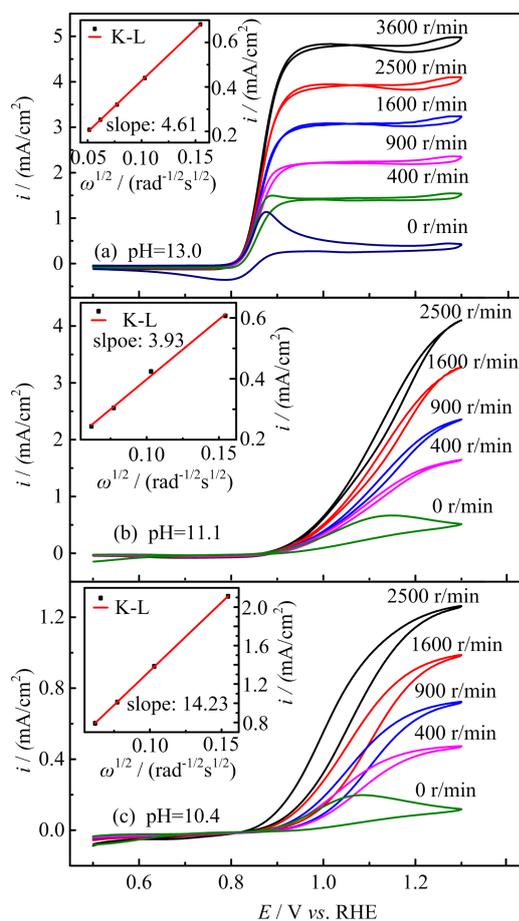
FIG. 2 Polarization curves for the oxidation of H_2O_2/HO_2^- on Au(111) electrode in 0.5 mol/L $NaClO_4$+2 mmol/L H_2O_2+x mmol/L NaOH with pH of (a) 13, (b) 11.1 and (c) 10.4 at various electrode rotation speeds, as indicated in the figure, scan rate: 50 mV/s. Inset in (a) shows the diffusion-limited current as a function of the root square of the electrode rotation speed.

potential. The diffusion-limited current for oxidation of H_2O_2 or HO_2^- is reached because the concentration of hydrogen peroxide is rather low (2 mmol/L). The i-E curve in the potential regime from 0.8 V to 0.9 V is quite close to the one limited by mass transport effect with a Tafel slope near the onset potential below 30 mV/dec. When reversing the potential scan direction at 1.3 V, the HPOOR current in the potential region from 1.3 V to 1.1 V is slightly smaller than that in the positive-going scan, while at lower potentials, the HPOOR current remains nearly the same as that in the positive-going potential scan for the cases with electrode rotation speed (ω) higher than 400 r/min.

For the cases with $\omega \leq 400$ r/min, the slight decrease of HPOOR current at $E > 0.9$ V is due to the fact that mass transport rate of H_2O_2 to the electrode surface is slower than the rate of its consumption. As a result, the H_2O_2 concentration as well as its concentration gradient decreases as the potential is made more positive.

The inset (FIG. 2) shows the diffusion-limited current plotted as a function of the square root of the electrode rotation speed, which displays a well-defined linear behavior. From the slope, 2 electrons are estimated to be transferred, confirming the complete oxidation of H_2O_2 on Au(111) electrode. For the cases in which the electrode rotation speed is higher than 400 r/min, barely any cathodic current is observed at 0.5 V$<E<$0.8 V (except the small double layer charging current) in the negative-going scan. This indicates that Au(111) is not active for the reduction of HO_2^- at these potentials, although the applied potential (*e.g.*, at 0.8 V) is ca. 0.8 V more negative than the thermodynamic equilibrium potential for the reduction of HO_2^- to OH^-. This is in contrast to the case of a Pt electrode, where the i-E curves for both HPOOR and HPORR are symmetric at around 0.8 V [6]. However, for the case at 0 r/min, an obvious cathodic peak is observed at ca. 0.8 V, which is attributed to the reduction of O_2 produced in the previous positive-going potential scan to HO_2^-. This is similar to the case with Au(100) [2, 7, 9]. When the electrode rotates, the rate at which O_2 leaves the electrode surface is higher than its readsorption and reduction. Hence, no current for its reduction is observed.

The general features for HPOOR on Au(111) in solutions with pH=11.1 and 10.4 are similar to that with pH=13. For all examined pHs, there is barely any current measured for $E < 0.8$ V. At $E > 0.83$ V, a net anodic current flows, which increases with electrode potential and electrode rotation speed. Furthermore, the i-E features in the subsequent, negative-going scan follow roughly that in the positive-going scan in all examined solutions. Besides such similarities, several significant differences are noticed: at the same potential, HPOOR current decreases significantly with the decrease of solution pH from 13 to 10. As a result, the slope of the i-E curve decreases, and the potential at which the plateau is reached shifts to higher potential. For the case with pH=10.4, the HPOOR current at 1.3 V is only ca. 1.25 mA/cm², which is ca. 1/4 of the diffusion-limited current detected at $E > 0.95$ V in solution with pH=13. The pH dependence of the i-E curves for HPOOR is seen more clearly in FIG. 3, where the i-E curves for HPOOR on Au(111) recorded under 2500 r/min in solutions with different pHs are shown. Compared with the case in 0.1 mol/L HClO₄, we found that in 0.1 mol/L NaOH the onset potential for HPOOR is ca. 0.2 V more negative. With the pH decrease of solution, although the onset potential does not show obvious positive shift, the Tafel slope displays a clear increase, which is more than 120 mV/dec in solution with pH=10.4. Furthermore, we found that in all solutions there is barely any HPORR activity on perfect Au(111) in the potential regime from 0.5 V to 0.8 V. This is probably because the interaction of H_2O_2 (or HO_2^-) with Au(111) is too weak, since the d-band center of Au(111) is ca. 3 eV lower than its Fermi level [3].

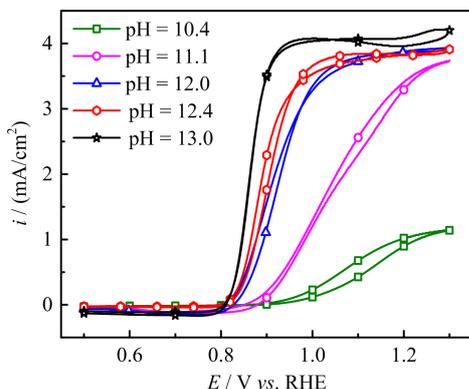In the following, we will focus on the pH effect on

FIG. 3 Polarization curves for the oxidation of H_2O_2 or HO_2^- on Au(111) in 0.5 mol/L $NaClO_4$+2 mmol/L H_2O_2 +x mmol/L NaOH. pH values are indicated in the figure. Electrode rotation speed: 2500 r/min, scan rate: 50 mV/s.

the HPOOR at a Au(111) electrode in alkaline media. Before discussing the origins of the pH effect on the HPOOR, we will first give an overview of how the concentrations of the reactants, as well as the equilibrium potential for HPOOR, change with the pH solution. When changing the solution pH, the following reactions will occur

$$H_2O_2 \rightleftharpoons HO_2^- + H^+ \qquad (1)$$
$$H_2O \rightleftharpoons OH^- + H^+ \qquad (2)$$
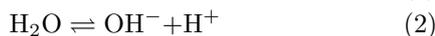
The pH-dependences of the H_2O_2 and HO_2^- concentration are:

$$[H_2O_2] = c_{\text{tot}} \frac{1}{1 + 10^{-(pK_a - pH)}} \qquad (3)$$

$$[HO_2^-] = c_{\text{tot}} \frac{10^{-(pK_a - pH)}}{1 + 10^{-(pK_a - pH)}} \qquad (4)$$

The pK_a of H_2O_2 is 11.8, the pH dependences of HO_2^- and H_2O_2 concentration in solutions prepared with 2 mmol/L H_2O_2 are plotted in FIG. 4(a). From FIG. 4(a), we see that when the pH is below 10, H_2O_2 is the main species, while with 10<pH<13, both HO_2^- and H_2O_2 exist in the solution. HPOOR may go through:

$$O_2 + 2H^+ + 2e^- \rightleftharpoons H_2O_2 \qquad (5)$$
$$O_2 + 2H_2O + 2e^- \rightleftharpoons H_2O_2 + 2OH^- \qquad (6)$$
$$O_2 + H_2O + 2e^- \rightleftharpoons HO_2^- + OH^- \qquad (7)$$

The equilibrium potentials for reactions (5), (6), and (7) are:

$$E_5 = E_5^0 + \frac{RT}{2F} \ln \frac{[O_2] \cdot [H^+]^2}{[H_2O_2]} \qquad (8)$$

$$E_6 = E_6^0 + \frac{RT}{2F} \ln \frac{[O_2]}{[H_2O_2][OH^-]^2} \qquad (9)$$

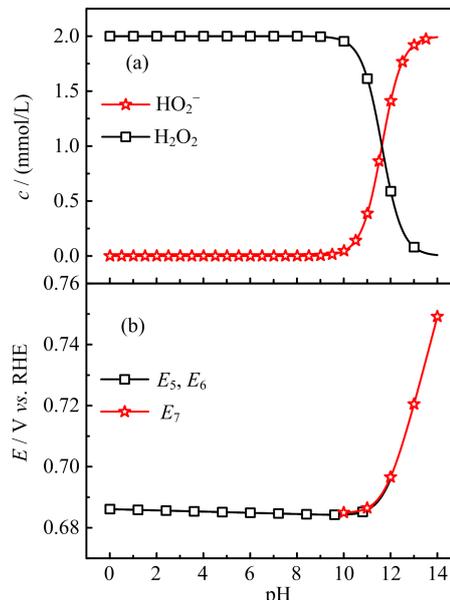$$E_7 = E_7^0 + \frac{RT}{2F} \ln \frac{[O_2]}{[HO_2^-][OH^-]} \qquad (10)$$

FIG. 4 (a) Concentration and (b) equilibrium potential for the oxidation of H_2O_2 and HO_2^- as a function of solution pH. The total concentration of H_2O_2+HO_2^- is 2 mmol/L.

Assuming that the concentration of O_2 near the electrode surface in all solutions is ca. 1.0×10^{-3} mol/L, the pH dependencies of the equilibrium potentials of reactions (5), (6) and (7) can be estimated. The results are plotted in FIG. 4(b).

When pH is smaller than 11.8, the dominant reactive species in the solution is H_2O_2. From FIG. 4(b), we see that equilibrium potential-pH relations for reactions (5) and (6) are identical. On the RHE scale it does not change with solution pH in the range from 0 to 12. For reaction (7) with HO_2^- and OH^- as reactants, its equilibrium potential increases with increasing solution pH. In the solutions with pH=10 and 11.8, the E_{eq} for reaction (7) are ca. 0.17 V and 0.06 V more negative than those for reaction (5) and reaction (6), respectively. This indicates that if we apply the same potential versus RHE, the driving forces for reactions (5) and (6), with H_2O_2 as reactant, are ca. 0.17 V and 0.06 V larger than that for reaction (7) with HO_2^- as reactant, respectively. However, the HPOOR rate we observed at lower pH is significantly smaller than that at higher pH. We think this is due to the low d-band center, which reduces the interaction between Au(111) and H_2O_2, hence the barrier for HPOOR through H_2O_2 as a reactive species is very high [9]. In contrast, at potentials where HPOOR occurs, the Au(111) surface is positively charged [14], and electrostatic interaction will facilitate the adsorption of HO_2^-. Therefore, the barrier for the oxidation of HO_2^- (*i.e.*, backward reaction of Eq.(7)) will be smaller than that for oxidation of H_2O_2 (back reaction of Eq.(5) and Eq.(6)). Under these circumstances, we think the major species to be discharged at the electrode is HO_2^-, which can be formed

from the dissociation of H_2O_2 near the electrode surface (reaction (1)).

IV. CONCLUSION

Hydrogen peroxide oxidation on Au(111) electrode in alkaline media (with pH from 10 to 13) has been investigated. We found that HPOOR activity increases with increasing the solution pH. HO_2^- is suggested to be the main reactive species for HPOOR in the alkaline media. Two possible origins may lead to the increase of HPOOR activity with solution pH increasing: (i) with the increase of solution pH, the concentrations of both reactants, $i.e.$, HO_2^- and OH^-, increase. As a result, the kinetics of HPOOR increase; (ii) at the same applied potential versus RHE, the overpotential for HPOOR through reaction (7) increases with increasing pH, which will also lead to increasing HPOOR activity with increasing solution pH. The significantly smaller HPOOR current in solutions with pH=10.4 and 11.1 is probably due to the concentrations of the two reactive species of reaction (7), $i.e.$, HO_2^- and OH^- are very small and the consumption of OH^- shifting the interfacial pH to smaller values, which further reduces the concentration of HO_2^- near the electrode surface.

V. ACKNOWLEDGEMENTS

[1] A. M. Gómez-Marín, R. Rizo, and J. M. Feliu, Catal. Sci. Technol. **4**, 1685 (2014).
[2] D. Mei, Z. Da He, Y. L. Zheng, D. C. Jiang, and Y. X. Chen, Phys. Chem. Chem. Phys. **16**, 13762 (2014).
[3] A. Ignaczak, R. Nazmutdinov, A. Goduljan, L. M. de Campos Pinto, F. Juarez, P. Quaino, E. Santos, and W. Schmickler, Nano. Energy **29**, 362 (2016).
[4] M. F. Li, L. W. Liao, D. F. Yuan, D. Mei, and Y. X. Chen, Electrochem. Acta **110**, 780 (2013).
[5] L. W. Liao, M. F. Li, J. Kang, D. Chen, Y. X. Chen, and S. Ye, J. Electroanal. Chem. **688**, 207 (2013).
[6] Y. Zheng, W. Chen, X. Q. Zuo, J. Cai, and Y. X. Chen, Electrochem. Commun. **73**, 38 (2016).
[7] Y. L. Zheng, D. Mei, Y. X. Chen, and S. Ye, Electrochem. Commun. **39**, 19 (2014).
[8] E. Sitta, A. M. Gómez-Marín, A. Aldaz, and J. M. Feliu, Electrochem. Commun. **33**, 39 (2013).
[9] Y. L. Zheng, J. Wei, and Y. X. Chen, J. Electrochem. **22**, 602 (2016).
[10] A. M. Gómez-Marín, A. Boronat, and J. M. Feliu, Russ. J. Electrochem. **53**, 1029 (2017).
[11] J. Clavilier, R. Faure, G. Guinet, and R. Durand, J. Electroanal. Chem. Interface **211**, 107 (1980).
[12] H. Angerstein-Kozlowska, B. Conway, A. Hamelin, and L. Stoicoviciu, J. Electroanal. Chem. Interface **228**, 429 (1987).
[13] U. Zhumaev, A. V. Rudnev, J. F. Li, A. Kuzume, T. H. Vu, and T. Wandlowski, Electrochem. Acta **112**, 853 (2013).
[14] U. Hamm, D. Kramer, R. Zhai, and D. Kolb, J. Electroanal. Chem. **414**, 85 (1996).